Journal of Applied Mathematics and Physics (ZAMP) 0044-2275/91/010109-13 \$ 1.50+0.20
Vol. 42, January 1991 

# Dynamical characteristics of decaying Lamb couples

By Gordon E. Swaters, Applied Mathematics Institute, Dept of Mathematics, also Institute for Earth and Planetary Physics, University of Alberta, Edmonton, Alberta, Canada T6G 2G1

## 1. Introduction

Swaters [1] introduced a simple multiple-scales asymptotic theory to describe the turbulent dissipation of the two-dimensional Lamb dipole vortex assuming a relatively small damping parameter. The Lamb couple or modon as this inertial dipole is sometimes referred to, is a ubiquitous feature in many experimental [2, 3] and numerical [4, 5] realizations of *two-dimensional turbulence* and plays a role in the double-cascade [6, 7, 8] concept where enstrophy and energy undergo blue and red cascades, respectively. In particular, it is believed that inertial dipole vortices similar to the Lamb couple may have a role to play in anomalous planetary-scale atmospheric circulation patterns such as blocking [9, 10, 11] or in describing the convective motions associated with anomalous heat transports in fusion containment devices [12]. However, very little is known about the stability of these nonlinear modes. It is of interest, therefore, to determine the dynamical characteristics of these solutions if they are subjected to weak but nonnegligible forcing.

The perturbation theory developed by Swaters assumed that the perturbed drift-vortex evolved in such a manner as to maintain globally-averaged enstrophy and energy balances. These transport equations were obtained rigorously as necessary solvability conditions on the first-order perturbation equations associated with a direct asymptotic expansion in integral powers of the damping parameter. As well, it was assumed that the Lamb modon "dispersion" relationship was also continuously maintained throughout the dissipation (at least during the main decay sequence). There were several interesting predictions that this perturbation theory implied and that should be confirmed by direct numerical simulation. For example, the asymptotic theory predicted that the "modon wavenumber" of the decaying Lamb couple was invariant and that the dipole radius did not dilate during the dissipation process. These properties are very different from the decay characteristics of the $\beta$-plane barotropic modon [13] and the Hasegawa-Mima modon [14] which have a monotonically increasing radius and concomitant decreasing wavenumber during the dissipation process. The principal purpose of this paper is to present a high-resolution numerical solution of the two-dimensional Navier-Stokes equations assuming a Lamb couple as an initial condition, and to compare the results of the Swaters perturbation theory with the results of the numerical simulation. We shall show that the agreement is very good.

Another important assumption in the perturbation theory is that the *non-analytic* linear functional relationship between the $O(1)$ stream function and vorticity fields in the Lamb modon is being continuously maintained throughout the decay. It has been suggested [12] that this is an unrealistic assumption in the perturbation theory. We shall present a time sequence of detailed stream function-vorticity scatter plots for the decaying Lamb couple to show that the non-analytic linear vorticity-stream function functional relationship is being continuously maintained to a high degree accuracy although some scatter does set in. However, we would like to immediately point out here that it is our opinion that if the magnitude of the external forcing becomes large in an appropriate sense, this adiabatic ansatz will probably fail. For example, see the scatter diagrams presented by McWilliams and Zabusky [15] for modon-modon interactions.

The plan of this paper is as follows. In Section 2 we will very briefly review the salient features of the perturbation theory presented in Ref. [1]. In Section 3 we shall describe the numerical procedure and present the comparison. The paper is summarized and some concluding remarks will be made in Section 4.

## 2. Description of the Asymptotic Theory

We write the scaled two-dimensional incompressible homogeneous Navier-Stokes equations with Rayleigh damping in the form

$$\Delta\varphi_t + J(\varphi, \Delta\varphi) = R^{-1}\Delta\varphi, \tag{2.1}$$

where $\varphi$ is the stream function [with corresponding velocity field $\boldsymbol{u} \equiv (u, v) \equiv \boldsymbol{e}_3 \boldsymbol{x} \nabla\varphi$], $\Delta \equiv \partial^2_{xx} + \partial^2_{yy}$, the Jacobian is given by $J(A, B) \equiv A_x B_y - B_x A_y$ (subscripts indicate differentiation), and $R$ is the "Reynolds number".

In the inviscid limit (i.e. $R \to \infty$) an exact nonlinear steadily-translating isolated eddy solution to (2.1) is the Lamb couple which can be written in the form

$$\varphi(x, y, t) = -a^2 c r^{-1} \sin(\theta) \quad r > a, \tag{2.2a}$$

$$\varphi(x, y, t) = [2ck^{-1} J_1(kr)/J_0(ka) - cr] \sin\theta \quad r < a, \tag{2.2b}$$

with the "dispersion" relation

$$J_1(ka) = 0, \tag{2.2c}$$

and where the co-moving polar coordinates $r^2 \equiv (x - ct)^2 + y^2$ and $\tan(\theta) \equiv y/(x - ct)$ have been introduced. The parameter $k$ is the eddy "wavenumber," $c$ is the translation speed, and $a$ is the eddy "boundary" between the *interior* $(r < a)$ and the *exterior* $(r > a)$ regions. The *ground-state* eddy dispersion relationship is given by

$$ka = j_{1,1}, \tag{2.3}$$

where $j_{1,1} \simeq 3.83171$ is the first non-trivial zero of the Bessel function $J_1(*)$.

It follows from (2.2a,b) that the nonanalytic linear stream function-vorticity relationship for the Lamb modon can be expressed in the form

$$\Delta\varphi = 0 \cdot (\varphi + cy) \quad r > a, \tag{2.4a}$$

$$\Delta\varphi = -k^2(\varphi + cy) \quad r < a. \tag{2.4b}$$

When the Reynolds number in (2.1) is relatively large but finite we can obtain an asymptotic solution for the decaying Lamb dipole in terms of the rapidly-varying phase variables

$$\xi \equiv x - R\int_0^{t/R} c(t')\,dt', \tag{2.5a}$$

$$y \equiv y, \tag{2.5b}$$

and the *slow* time variable

$$T \equiv t/R. \tag{2.5c}$$

Substitution of (2.4) into (2.1) gives

$$J(\varphi + cy, \Delta\varphi) = R^{-1}\Delta\varphi - R^{-1}\Delta\varphi_T, \tag{2.6}$$

where the Jacobian is understood to be with respect to $\xi$ and $y$, and $\Delta \equiv \partial^2_{\xi\xi} + \partial^2_{yy}$.

The remaining details are straight forward (see [1]). Equation (2.6) is solved with an expansion of the form

$$\varphi \sim \varphi^{(0)}(\xi, y; T) + R^{-1}\varphi^{(1)}(\xi, y; T) + R^{-2}\varphi^{(2)}(\xi, y; T) + \cdots. \tag{2.7}$$

Substitution of (2.7) into (2.6) will lead to a hierarchy of partial differential equations. The solution to the $O(1)$ problem is taken to be the Lamb couple (2.2) written with respect to the co-moving phase variables in (2.5). The adiabatic *ansatz* is that $c \equiv c(T)$, $a \equiv a(T)$ and $k \equiv k(T)$ such that the dispersion relationship (2.2c) remains continuously satisfied.

Examination of the homogeneous adjoint equation associated with the $O(R^{-1})$ problem leads to the following *solvability conditions* on the $O(1)$ solutions

$$\partial_T \iint_{\mathbb{R}^2} (\Delta\varphi^{(0)})^2 = 2 \iint_{\mathbb{R}^2} \Delta\varphi^{(0)}\Delta\varphi^{(0)}, \tag{2.8a}$$

$$\partial_T \iint_{\mathbb{R}^2} \varphi^{(0)}\Delta\varphi^{(0)} = 2 \iint_{\mathbb{R}^2} \varphi^{(0)}\Delta\varphi^{(0)}, \tag{2.8b}$$

which when evaluated yield the *transport equations*

$$c_T = -c, \tag{2.9a}$$

$$(ac)_T = -ac, \tag{2.9b}$$

for the ground-state Lamb dipole. The solution to (2.9) and (2.2) is simply

$$a(T) \equiv a_0, \tag{2.10a}$$

$$k(T) \equiv k_0 \equiv j_{1,1}/a_0, \tag{2.10b}$$

$$c(T) \equiv c_0 \exp[-T], \tag{2.10c}$$

where the zero subscript denotes the value at $T \equiv 0$. Hence, we see immediately that the theory predicts that the spatial structure of the decaying Lamb couple is constant.

## 3. Comparison between theory and numerical simulation

There are several important predictions of the above theory that can be directly compared with a numerical simulation. The solutions (2.9) will imply that the $e$-folding decay time scale in the amplitude of both the stream function and vorticity fields is time independent and is set by the initial Lamb wavenumber. As well, since $a(T)$ and $k(T)$ are invariant in time, the coordinates of the extrema in the vorticity and stream function fields relative to the co-moving frame should be time independent. If the Lamb dipole was dilating throughout the decay process, one should expect to see the radial coordinate of the extrema monotonically increase. A list of the computed diagonistic variables that we will present is diplayed in Table 1.

The numerical scheme adopted for (2.1) is as follows. The vorticity equation is split into the coupled system

$$q_t + J(\varphi, q) = \frac{1}{R} q, \tag{3.1}$$

$$\Delta\varphi = q. \tag{3.2}$$

Table 1
Definition of symbols used in the diagonistic calculations.

| | |
|---|---|
| $X_c(t) \equiv R \int_0^{t/R} c(\tau)\,d\tau$ | Position of the center of the decaying Lamb couple. |
| $En(t)/En(0) \equiv \dfrac{\int_{-\infty}^{\infty}\int_{-\infty}^{\infty} [\nabla\varphi \cdot \nabla\varphi](\xi, y; t/R)\,d\xi\,dy}{\int_{-\infty}^{\infty}\int_{-\infty}^{\infty} [\nabla\varphi \cdot \nabla\varphi](\xi, y; 0)\,d\xi\,dy}$ | The time-dependent area-integrated energy normalized by its initial value. |
| $Es(t)/Es(0) \equiv \dfrac{\int_{-\infty}^{\infty}\int_{-\infty}^{\infty} [(\Delta\varphi)^2](\xi, y; t/R)\,d\xi\,dy}{\int_{-\infty}^{\infty}\int_{-\infty}^{\infty} [(\Delta\varphi)^2](\xi, y; 0)\,d\xi\,dy}$ | The time-dependent area-integrated enstrophy normalized by its initial value. |
| $vml(t)$ | Radial coordinate of the maximum in the vorticity $\lvert\Delta\varphi(r, \theta; t/R)\rvert$ with $\theta = \pi/2$. |
| $vm(t)/vm(0) \equiv \dfrac{\max[\lvert\Delta\varphi(vml, \pi/2; t/R)\rvert]}{\max[\lvert\Delta\varphi(vml(t=0), \pi/2; 0)\rvert]}$ | The time-dependent magnitude of the maximum vorticity normalized by its initial value. |
| $sml(t)$ | Radial coordinate of the maximum in the stream function $\lvert\varphi(r, \theta; t/R)\rvert$ with $\theta = \pi/2$. |
| $am(t)/sm(0) \equiv \dfrac{\max[\lvert\varphi(sml, \pi/2; t/R)\rvert]}{\max[\lvert\varphi(sml(t=0), \pi/2; 0)\rvert]}$ | The time-dependent magnitude of the maximum in the stream function normalized by its initial value. |

The vorticity, $q(x, y, t)$, is integrated forward in time using a 2nd-order symplectic leapfrog procedure in which the Jacobian is finite-difference with the Arakawa [16] (see also McWilliams et al. [17]) scheme which preserves skew-symmetry, and energy and enstrophy conservation. The updated stream function is then obtained from the Poisson problem (3.2) using a direct solver. The problem was also solved in a $128 \times 128$ doubly-periodic square domain, in which each side had a length of ten nondimensional units. It has been recently shown by Browning and Kreiss [18] that in the computation of two-dimensional turbulence, 2nd-order $128 \times 128$ difference schemes give qualitatively similar results as $64 \times 64$ spectral methods for $t \leqslant 200$. The initial nondimensional Lamb radius was set to one. Thus the finite-difference scheme had a grid spacing of about $\delta_x = \delta_y \equiv 0.0787$ units or about 25.4 grid points per Lamb radius. McWilliams et al. [17] have shown that with this resolution the numerical translation speed of the Lamb drift-vortex will be well within 5% of the true translation speed. The nondimensional time step was chosen to be $5 \times 10^{-3}$. With these finite difference parameters the linearized *Courant-Friedrichs-Lewy* stability criteria was always satisfied for (3.1). Finally, because the domain was doubly-periodic we smoothed the initial data near the domain boundaries according to the recipe in Ref. [17] (see also Ref. [14]). For our simulation we set $a_0 = 1.0$, $c_0 = 1.0$ and $k_0 = 3.83171$ and $R \equiv 10^2$.

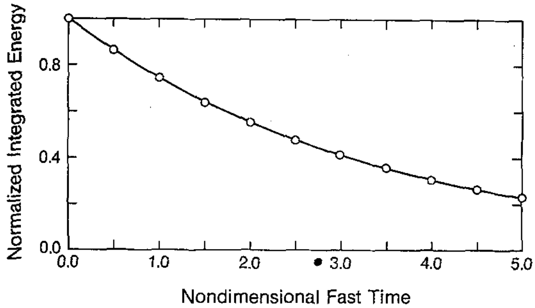


Figure 1a
Decay in the normalized globally-averaged energy (see Table 1). The solid line is the theoretical prediction and the open circles are the numerically determined values.

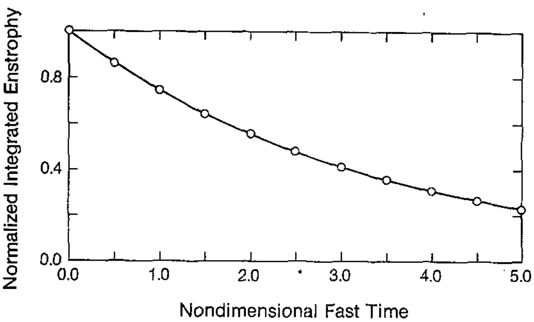


Figure 1b
Decay in the normalized globally-averaged enstrophy (see Table 1). The solid line and circles are as described in Figure 1a.

The comparison is summarized in Figures 1–5. In Figures 1a and 1b we present the comparison between the decay in the normalized globally-averaged energy and enstrophy between the theory and the numerical simulation, respectively. The theory predicts that the decay is a simple exponential with a constant $e$-folding fast time scale of $R/2$. The numerically determined integrated energy and enstrophy was obtained by simple summing $-q\varphi\delta_x\delta_y$ and $q^2\delta_x\delta_y$ over all grid points, respectively and normalizing by the initial value. It is clear from Figures 1a and 1b that the integrated decay properties are reproduced very accurately.

Figure 2 is a comparison between the predicted location of the $x$-coordinate associated with the propagating Lamb couple and the numerically determined position. The numerically determined location was obtained by tracking the $x$ and $y$ coordinates of the relative extrema in the stream function and vorticity fields. These coordinates and the extrema values were obtained by a quadratic interpolation procedure.

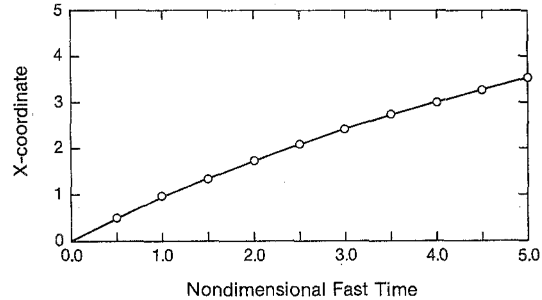


Figure 2
The $x$-coordinate of the travelling Lamb modon (see Table 1). The solid line and circles are as described in Figure 1a.

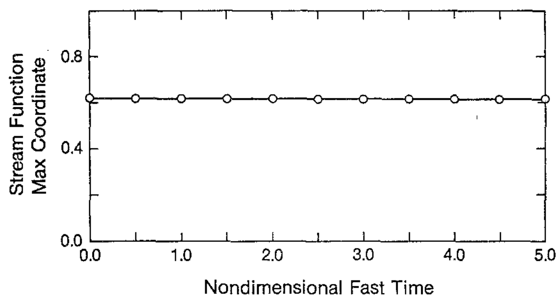


Figure 3a
The radial coordinate of the stream function maximum (see Table 1). The solid line and circles are as described in Figure 1a.

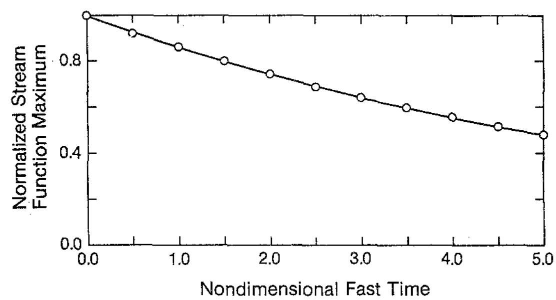


Figure 3b
The decay in the normalized maximum of the stream function field (see Table 1). The solid line and circles are as described in Figure 1a.

Figures 3a,b and 4a,b depict the radial coordinate of the stream function and vorticity maximum and its magnitude. Because the theory predicts that the Lamb wavenumber and radius is temporally invariant, it follows that the theory predicts that the radial coordinate in the extrema will also be invariant. Figures 3a and 4a show that the numerical simulation retains this property. This decay characteristic of the Lamb couple is

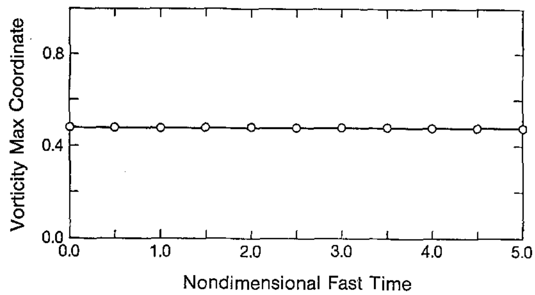


Figure 4a
The radial coordinate of the vorticity maximum (see Table 1). The solid line and circles are as described in Figure 1a.

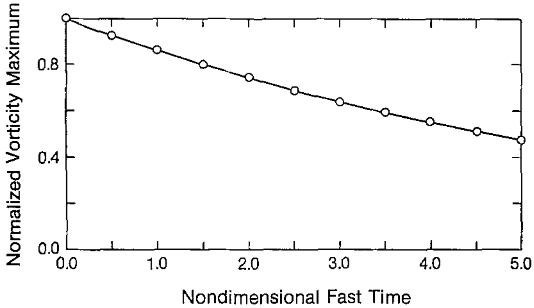


Figure 4b
The decay in the normalized maximum of the vorticity field (see Table 1). The solid line and circles are as described in Figure 1a.

different from the dilation seen in the dissipating modon solutions in $\beta$-plane dynamics [13, 14, 17]. We attribute this difference to the fact that in the $\beta$-plane modon the spatial scale (i.e, the modon wavenumber and radius) is parametrically coupled to the translation speed in the $\beta$-plane modon dispersion relationship and in the Lamb couple this dependency does not occur because of the absence of a background vorticity gradient in the exterior region (i.e., $r > a$). The decay in the amplitude of the vorticity and stream function fields is also exponential.

In Figure 5a–f we present a time sequence of vorticity-stream function scatter diagrams for $t = 0, 0, 5, 1.0, \ldots 5.0$, respectively. The translation speed used in the co-moving stream function was obtained from the numerical simulation. The adiabatic theory we have predicted here has explicitly assumed that the nonanalytic linear functional relationships between the vorticity and the stream-function (2,4a,b) is being continuously maintained during the decay. Figure 5a–f show that this relationship is in fact being maintained throughout the main decay sequence to a very high degree. We shall comment on this property in Section 4.

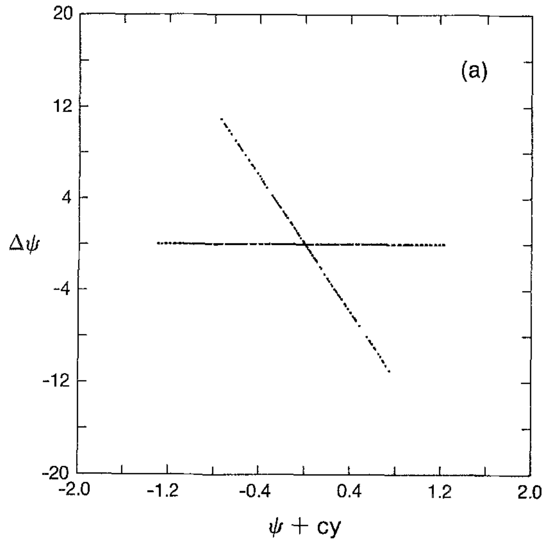


Figure 5a

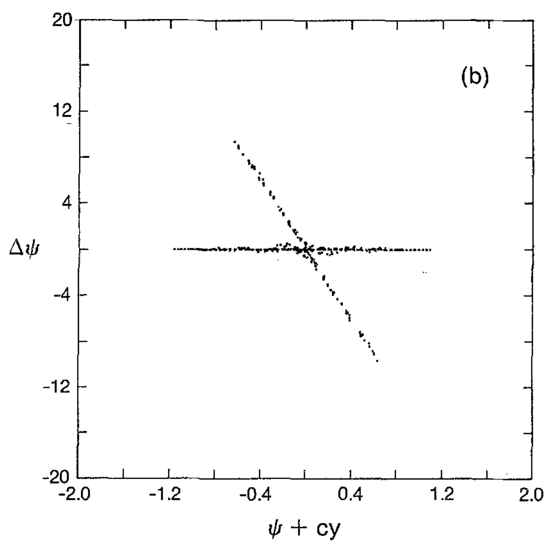


Figure 5b

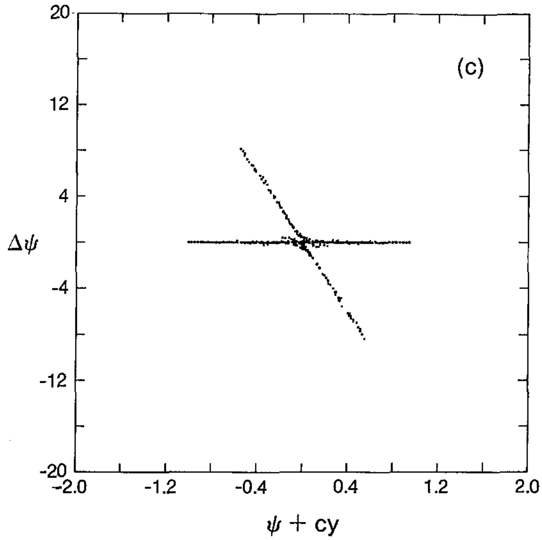


Figure 5c

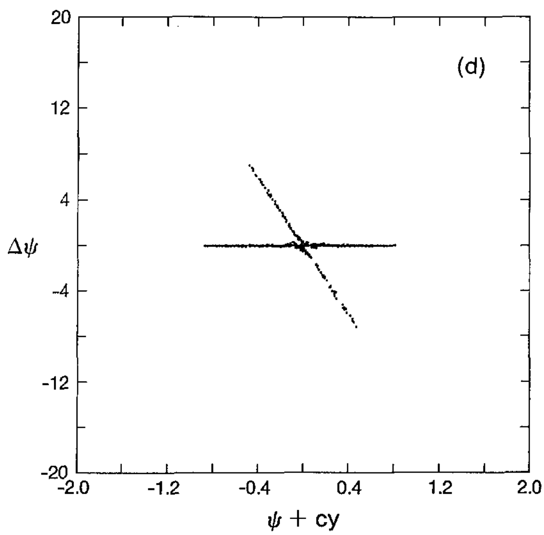


Figure 5d

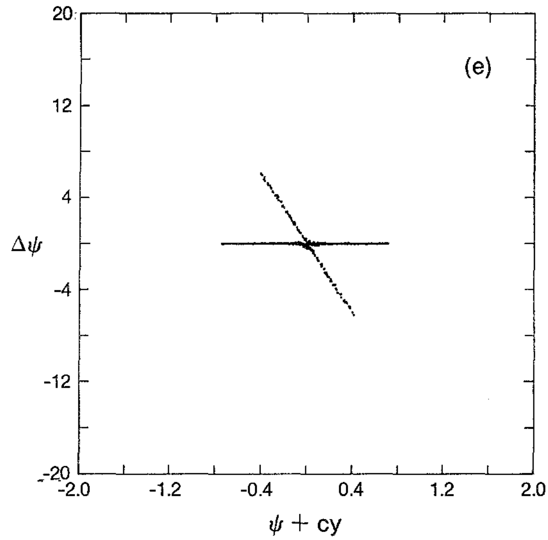


Figure 5e

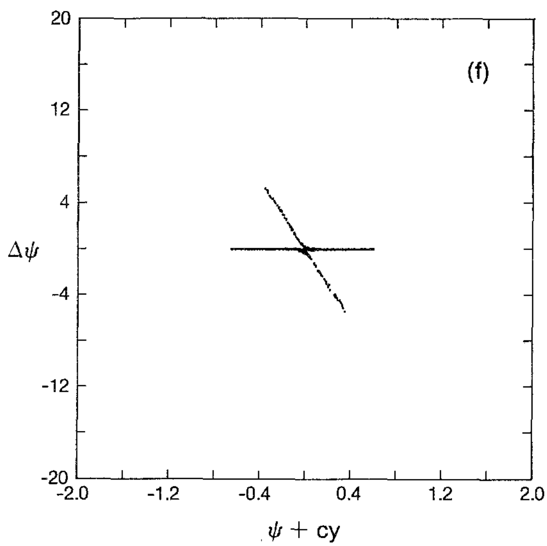


Figure 5f

Figure 5
Time-series scatter diagrams of the vorticity $\Delta\varphi$ versus the co-moving streamlines $\varphi + cy$ for the numerical simulation. The panels $a$, $b$, $c$, $d$, $e$ and $f$ correspond to $t = 0$, 1, 2, 3, 4 and 5, respectively. The negatively sloped curve corresponds to points in the interior ($r < a$) region, and the flat curve corresponds to points in the exterior ($r > a$) region.

## 4. Summary and concluding remarks

A comparison has been presented between a high-resolution numerical simulation of a frictionally decaying Lamb couple and a multiple-scale asymptotic theory proposed previously [1]. Not only are global properties, such as the predicted decay in the area-integrated energy and enstrophy accurately reproduced, but also "local" properties such as the theoretically predicted temporal invariance of the spatial structure (i.e., the Lamb couple wavenumber and radius) have been numerically confirmed. This means that the decay characteristics of the Lamb mode is quite different than the decay characteristics of $\beta$-plane modons. We have also presented a detailed time-series of vorticity-stream function scatter diagrams to provide numerical confirmation of the adiabatic ansatz which has been explicitly assumed in the adiabatic perturbation theory.

The point has been made [12], that there is no *a priori* reason to believe that the non-analytic functional relationships between the stream function and vorticity fields ought to be maintained during a period of perturbed evolution. We believe, however, that if the forcing is weak enough in an appropriate sense these nonlinear modes will respond adiabatically. We have made the point in the context of the Hasegawa-Mima or equivalent-barotropic modon [14], that these nonlinear modes satisfy the first-order necessary conditions for the variational problem determined by an enstrophy constrained by the energy pseudo-Hamiltonian. If these modes are examples of minimum enstrophy vortices in two-dimensional turbulence [19], then it would seem plausible that during a period of "small-amplitude" forcing an adiabatic evolution would occur at least initially. There are important caveats to be made however. Under "large-amplitude" forcing the adiabatic ansatz will probably completely fail as it does during vortex-vortex interactions [15] or partially fail as it does in modon-topographic interactions [20].

## Acknowledgements

Preparation of this paper was supported in part by Operating Research Grants awarded by the Natural Sciences and Engineering Research Council of Canada, and Science Subventions awarded by the Atmospheric Environment Service of Canada, and the Department of Fisheries and Oceans of Canada.

#### References

[1] Swaters, G. E., *Viscous modulation of the Lamb dipole vortex*. Phys. Fluids *31*, 2745–2747 (1988).

**References**


[1] Swaters, G. E., *Viscous modulation of the Lamb dipole vortex.* Phys. Fluids *31*, 2745–2747 (1988).

[2] Flierl, G. R., M. E. Stern, and J. A. Whitehead, *The physical significance of modons: Laboratory experiments and general integral constraints*, Dyn. Atmos. Oceans *7*, 233–263 (1983).

[3] Hopfinger, E., F. Browand, and Y. Cagne, J. Fluid Mech. *125*, (1983).

[4] Babiano, A., C. Basdevant, B. Legras, and R. Sadourny, *Vorticity and passive-scalar dynamics in two-dimensional turbulence.* J. Fluid Mech. *183*, 379–397 (1987).

[5] Legras, B., P. Santangelo, and R. Benzi, *High-resolution numerical experiments for forced two-dimensional turbulence.* Europhys. Lett *5*, 37–42 (1988).

[6] Kraichnan, R. H., *Inertial ranges in two-dimensional turbulence.* Phys. Fluids *10*, 1417–1423 (1967).

[7] Leith, C. E., *Diffusion approximation for two-dimensional turbulence.* Phys. Fluids *11*, 671–673 (1968).

[8] Batchelor, G. K., *Computation of the energy spectrum in homogeneous two-dimensional turbulence.* Phys. Fluids Suppl. *12*, 233 (1969).

[9] McWilliams, J. C., *An application of equivalent modons to atmospheric blocking.* Dyn. Atmos. Oceans *5*, 43–66 (1980).

[10] Haines, K. and J. Marshall, *Eddy-forced coherent structures as a prototype of atmospheric blocking.* Q. J. R. Meteorol. Soc. *113*, 681–704 (1987).

[11] Haines, K., *Baroclinic modons as prototypes for atmospheric blocking.* J. Atmos. Sci. *46*, 3202–3218 (1989).

[12] Nycander, J., *New stationary vortex solutions of the Hasegawa-Mima equation.* J. Plasma Physics *39*, 413–430 (1988).

[13] Swaters, G. E. and G. R. Flierl, *Ekman dissipation of a barotropic modon*, In *Mesoscale/Synoptic Coherent Structures in Geophysical Turbulence* (J. C. J. Nihoul and B. M. Jamart, eds.), Elsevier Press, pp. 149–165, 1989.

[14] Swaters, G. E., *A perturbation theory for the solitary drift-vortex solutions of the Hasegawa-Mima equation.* J. Plasma Physics *41*, 523–539 (1989).

[15] McWilliams, J. C. and N. J. Zabusky, *Interactions of isolated vortices, I: Modons colliding with modons.* Geophys. Astrophys. Fluid Dynamics *19*, 207–227 (1982).

[16] Arakawa, A., *Computational design for long term numerical integration of the equations of fluid motion: Two dimensional incompressible flow. Part 1.* J. Computing Phys. *1*, 119–143 (1966).

[17] McWilliams, J. C., G. R. Flierl, V. O. Larichev and G. M. Reznik, *Numerical studies of barotropic modons.* Dyn. Atmos. Oceans *5*, 219–238 (1981).

[18] Browing, G. L. and H.-O. Kreiss, *Comparison of numerical methods for the calculation of two-dimensional turbulence.* Math. Comp. *52*, 369–388 (1989).

[19] Leith, C. E., *Minimum enstrophy vortices.* Phys. Fluids *27*, 1388–1395 (1984).

[20] Swaters, G. E., *Barotropic modon propagation over slowly-varying topography.* Geophys. Astrophys. Fluid Dynamics *36*, 85–113 (1986). Carnevale, G. F., G. K. Vallis, R. Purini, M. Briscoline, *Propagation of barotropic modons over topography.* Geophys. Astrophys. Fluid Dynamics *41*, 45–101 (1988).



**Abstract**

A multiple-scale adiabatic asymptotic theory is developed to describe the dissipation of the solitary Lamb couple or modon solutions of the two-dimensional Navier-Stokes equations. The transport equations describing the evolution of the Lamb couple are obtained as solvability conditions for a direct asymptotic expansion assuming a relatively large but finite Reynolds number and are equivalent to globally-integrated leading-order enstrophy and energy balances. The asymptotic theory predicts that the spectral or spatial characteristics of the decaying Lamb couple are temporally invariant and that there is a simple exponential decay in the amplitude and translation speed. We compare the predictions of the theory with a high-resolution numerical simulation. The global and local predictions of the theory and the results of the numerical simulation are in very good agreement. As well, we present a time-series of vorticity-stream function scatter diagrams as derived from the numerical simulation to show that the *non-analytic* linear vorticity-stream function relationship is being continuously maintained during the perturbed evolution of the Lamb couple.


(Received: January 2, 1990)